High Performance Amorphous Metallated π-Conjugated Polymers for Field-Effect Transistors and Polymer Solar Cells

Nam Seob Baek, Steven K. Hau, Hin-Lap Yip, Orb Acton, Kung-Shih Chen, and Alex K.-Y. Jen*

Department of Materials Science and Engineering, University of Washington, Seattle, Washington 98195-2120

Received June 16, 2008
Revised Manuscript Received August 8, 2008

Solution-processible organic field-effect transistors (OFETs) and organic photovoltaics (OPVs) have been extensively investigated due to their potential for low cost, large area, and lightweight electronic and optoelectronic applications.[1] One of the key enabling materials for OFETs and OPVs is π-conjugated semiconducting polymers with high charge carrier mobility and good processability. There are two approaches for the development of high-performance semiconducting polymers. The first one is to design materials with enhanced order through self-organization. The strong $\pi-\pi$ interactions in these polymers enables fast in-plane charge transport, leading to hole mobilities of 0.01 to 0.6 $cm^2\ V^{-1}\ s^{-1}$.[2] However, the performance of these systems is strongly dependent on the post-treatments[3] and the structural regioregularity of the polymers,[4] which increases the complexity for device processing. The alternative approach is to produce amorphous polymer thin films with a uniform path for charge transport.[5] Charge carrier mobility in this system is usually lower than that of the polycrystalline polymers due to the lack of band transport. The best reported field-effect mobility for the amorphous system is 6.1×10^{-3} $cm^2\ V^{-1}\ s^{-1}$ from a large bandgap polytriarylamine derivative.[6] Here we report the design and synthesis of a series of amorphous metallated π-conjugated polymers that show field-effect hole mobility up to 1.0×10^{-2} $cm^2\ V^{-1}\ s^{-1}$. In addition, their small bandgap and high extinction coefficient properties enable them to be used for high-performance OPVs.

Scheme 1. Metallated Conjugated Polymers

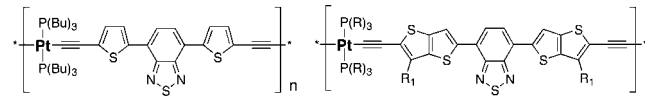

P1

R= Bu and R_1= H, P2
R= Bu and R_1= C_8H_{17}, P3
R= Et and R_1= C_8H_{17}, P4

The generally adapted strategy in designing low-bandgap conjugated polymers is to alternate the electron-rich and the electron-deficient units on the polymer backbone. Several low-bandgap polymers developed based on this principle have resulted in OPVs with efficiency of 2−5%.[7] Another approach is to introduce suitable organometallic donor moieties into the polymer main chain.[8] The complexation of an electron-donating transition metal (Pt) ion into the polymer main chain was reported to enhance the intrachain charge transport of π-conjugated polymers.[8,9] When Pt metal is conjugated with an alkyne unit, the d-orbitals (d_{xy} and d_{xz}) of the Pt overlaps with the p-orbitals (π_y* and π_z*) of the alkyne unit leading to the enhancement of π-electron delocalization along the polymer chain.[10] Previously, a Pt(II)-polymer based on 4,7-di-2′-thienyl-2,1,3-benzothiadiazole (**P1**) had been employed in a bulk heterojunction solar cell showing high power conversion efficiency (PCE) and moderate hole mobility.[8] Using a similar approach, we developed a series of Pt-based polymers derived from **P1** which show dramatically improved charge transporting properties. The synthesis of the bis-terminal alkyne monomer and the metallated conjugated polymers used in this study are summarized in Figure S1 (Supporting Information).

The bis-terminal alkyne unit was coupled with the *trans*-dichlorobis(trialkylphosphine) platinum(II) (*trans*-$PtCl_2(PR_3)_2$, R = C_2H_5 or C_4H_9) unit through the dehydrohalogenation method to give metallated conjugated polymers as shown in Scheme 1. The resulting polymers were purified by a Soxhlet apparatus with hexane and reprecipitated in MeOH. The two trialkylphosphine ligands on the platinum atom are used to improve the solubility and stability of the *trans* platinum(II) compound while the optical and electrical properties are tuned by coupling the platinum compound with a thiophene (T)- or thieno[3,2-*b*]thiophene (TT)-connected 2,1,3-benzothiodiazole. The resulting polymers exhibit λ_{max} at 587−611 nm in the solid state (Figure 1 and Table 1), which is attributed to the intramolecular charge transfer between the donor and the acceptor.[10] The electrochemical

(1) Zaumseil, J.; Sirringhaus, H. *Chem. Rev.* **2007**, *107*, 1296. Günes, S.; Neugebauer, H.; Sariciftci, N. S. *Chem. Rev.* **2007**, *107*, 1324.
(2) Sirringhaus, H.; Tessler, N.; Friend, R. H. *Science* **1998**, *280*, 1741. Sirringhaus, H.; Brown, P. J.; Friend, R. H.; Nielsen, M. M.; Bechgaard, K.; Langeveld-Voss, B. M. W.; Spiering, A. J. H.; Janssen, R. A. J.; Meijer, E. W.; Herwig, P.; deLeeuw, D. M. *Nature* **1999**, *401*, 685. Mcculloch, I.; Heeney, M.; Bailey, C.; Genevicius, K.; Macdonald, I.; Shkunov, M.; Sparrowe, D.; Tierney, S.; Wagner, R.; Zhang, W.; Chabinyc, M. L.; Kline, R. J.; Mcgehee, M. D.; Toney, M. F. *Nat. Mater.* **2006**, *5*, 328.
(3) Bao, Z.; Dodabalapur, A.; Lovinger, A. *Appl. Phys. Lett.* **1996**, *69*, 4108. Sirringhaus, H.; Wilson, R. J.; Friend, R. H.; Inbasekaran, M.; Wu, W.; Woo, E. P.; Grell, M.; Bradley, D. D. C. *Appl. Phys. Lett.* **2000**, *77*, 406. Li, G.; Shrotriya, V.; Huang, J. S.; Yao, Y.; Moriarty, T.; Emery, K.; Yang, Y. *Nat. Mater.* **2005**, *4*, 864.
(4) Kim, Y. K.; Cook, S.; Tuladhar, S. M.; Choulis, S. A.; Nelson, J.; Durrant, J. R.; Bradley, D. D. C.; Giles, M.; Mcculloch, I.; Ha, C.-S.; Ree, M. *Nat. Mater.* **2006**, *5*, 197.
(5) Sirringhaus, H. *Adv. Mater.* **2005**, *17*, 2411.
(6) Veres, J.; Ogier, S.; Lloyd, G.; de Leeuw, D. *Chem. Mater.* **2004**, *16*, 4543.
(7) Mühlbacher, D.; Scharber, M.; Morana, M.; Zhu, Z.; Waller, D.; Gaudiana, R.; Brabec, C. J. *Adv. Mater.* **2006**, *18*, 2884. Peet, J.; Kim, J. Y.; Coates, N. E.; Ma, W. L.; Moses, D.; Heeger, A. J.; Bazan, G. C. *Nat. Mater.* **2007**, *6*, 497.
(8) Wong, W.-Y.; Wang, X.-Z.; He, Z.; Djuric, A. B.; Yip, C.-T.; Cheung, K.-Y.; Wang, H.; Mak; C. S. K.; Chan, W.-K. *Nat. Mater.* **2007**, *6*, 521. Wong, W.-Y.; Wang, X.-Z.; He, Z.; Chan, K.-K.; Djuric, A. B.; Cheung, K.-Y.; Yip, C.-T.; Ng, A. M.-C.; Xi, Y. Y.; Mak, C. S. K.; Chan, W.-K. *J. Am. Chem. Soc.* **2007**, *129*, 14372.
(9) Schull, T. L.; Kushmerick, J. G.; Patterson, C. H.; George, C.; Moore, M. H.; Pollack, S. K.; Shashidhar, R. *J. Am. Chem. Soc.* **2003**, *1*, 25–3202.
(10) Masai, H.; Sonogashira, K.; Hagihara, N. *Bull. Chem. Soc. Jpn.* **1971**, *44*, 2226.

10.1021/cm8016424 CCC: $40.75
Published on Web 08/28/2008

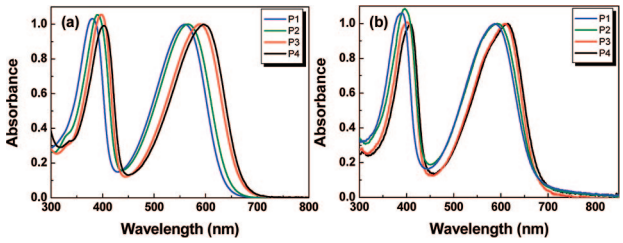

Figure 1. UV−vis absorption spectra of metallated conjugated polymers in CH_2Cl_2 solution (a) and solid state (b).

properties of the resulting polymers were studied by cyclic voltammetry with a three electrode cell in a 0.1 M solution of tetrabutylammonium hexafluorophosphate (Bu_4NPF_6) in CH_2Cl_2 (Figure S2, Supporting Information).

The results from the electrochemical and UV−vis absorption studies reveal that the bandgap of these polymers is in the range of 1.81−1.85 eV. The versatility of metallated π-conjugated polymers as a semiconducting polymer was demonstrated by measuring its charge mobility using an OFET configuration. A top contact, bottom gate OFET device structure was used, with heavily n-doped Si used as the gate, 300 nm SiO_2 modified with octadecyltrichlorosilane (OTS) as the dielectric, and vacuum deposited gold as source and drain electrodes. To investigate the structure−property relationship of these polymers, we systematically incorporated different heterocyclic units into the polymer backbone. By incorporating the more structurally rigid TT unit in **P2** compared to **P1**, the hole mobility and the on/off ratio significantly improved from 6.1×10^{-5} cm^2 V^{-1} s^{-1} and $\sim 10^2$ to 1.5×10^{-3} cm^2 V^{-1} s^{-1} and $\sim 10^4$, respectively (Figure S3, Supporting Information).

This more rigid structure enhances the electron coupling between the donor and the acceptor units along the polymer backbone.[11] By adding an alkyl chain on the TT moiety in **P3** and **P4**, the hole mobility is further improved to 1.0×10^{-2} cm^2 V^{-1} s^{-1}. Although alkyl chains typically promote packing of polymer chains via face-to-face stacking and improve intermolecular charge transport,[2] these polymers show amorphous thin film characteristics due to the steric hindrance between the bulky $-Pt(PR_3)_2-$ groups. To confirm the amorphous nature of the resulting polymers, we preformed X-ray diffraction analysis of polymers, **P1**−**P4** cast from chloroform onto silicon with native oxide substrates (Figure S4, Supporting Information). No diffraction peaks were observed in the cast films except for a broad peak at ∼4.5−6° and a second smaller peak at ∼8−9° which are attributed to the spectral reflection off the native oxide layer of the silicon substrate. Differential scanning calorimetry measurements show no apparent transition also indicating the amorphous nature of the polymers (Figure S5, Supporting Information). In addition, there are no significant changes in the absorption spectrum and morphology of spin-casted polymer films before and after annealing at 150 °C for 10 min, confirming the amorphous nature of the conjugated polymers.[12] Despite its amorphous nature, **P3** and **P4** show good charge transporting property. By decreasing the side-chain length of the phosphine ligand (PEt_3), the hole mobility of **P4** is slightly increased. This is probably due to the reduced steric hindrance between two adjacent alkyl side chains. The current−voltage characteristic of the **P4** OFET is shown in Figure 2. The hole mobility of **P4** in the saturation regime was 8.9×10^{-3} cm^2 V^{-1} s^{-1} based on the average of over 10 devices tested under ambient conditions. The best field-effect hole mobility reached 1.0×10^{-2} cm^2 V^{-1} s^{-1}. The OFETs showed a sharp turn on with a low subthreshold swing of approximately 1 V/decade and high on/off current ratio of $>10^6$. These results also revealed that *trans*-bistrialkylphosphine Pt(II)[9] and alkylthieno-[3,2-*b*]thiophene[2] unit strongly enhanced the charge transporting property of the conjugated polymer. This opens up the possibility for a new class of solution-processible semiconducting polymers for high performance OFETs without the need of post-processing.

Solar cell performance was investigated due to the suitable absorbance and charge transporting properties in these polymers. The representative characteristics of the solar cells are listed in Table 2. The bulk heterojunction solar cells had a layered structure of glass/ITO/PEDOT-PSS/polymer:PCBM or $PC_{71}BM$/LiF/Al. To optimize the performance of the cells, a series of devices were fabricated from chloroform (Table 2) and 1,2-dichlorobenzene (Table S1 and Figure S6, Supporting Information) varying the weight ratios of polymer:PCBM or $PC_{71}BM$. The optimum performance is obtained with devices having an active layer thickness of ∼80 nm with a 1:4 weight ratio of polymer:PCBM or $PC_{71}BM$. Using a lower fullerene ratio (1:1 and 1:2 w/w ratio) in the blend leads to a reduction in the short circuit current density due to the inefficient charge separation and transport property, resulting in relatively low power conversion efficiencies. After increasing the fullerene ratio, the device exhibits pronounced improvement. It should be noted that the effciency of the **P1**:PCBM system is lower than the reported results in literature under similar processing conditions.[8] However, a 1:4 weight ratio of **P4**:$PC_{71}BM$ system as shown in Figure 3 gave the best performance as compared to the others under the same processing conditions. AFM images (Figure 4) show a relatively smooth surface after processing the blend films (1:4 w/w ratio) from chloroform except for the **P1**:$PCB_{71}M$ which shows large phase segregration.

The improvement in solar cell performance from $PC_{71}BM$ compared to PCBM as the acceptor in these polymers can be attributed to the better absorbance and charge transport properties from $PC_{71}BM$.[14] Under the same processing

(11) Grozem, F. C.; van Duijnen, P. Th.; Berlin, Y. A.; Ratner, M. A.; Siebbeles, L. D. A. *J. Phys. Chem. B* **2002**, *106*, 7791. Grozema, F. C.; Houarner-Rassin, C.; Prins, P.; Siebbeles, L. D. A.; Anderson, H. L. *J. Am. Chem. Soc.* **2007**, *129*, 13370.

(12) Alexander, L. E. *X-Ray Diffraction Methodsin Polymer Science*; John Wiley: New York, 1969; p 43. Kaafarani, B. R.; Kondo, T.; Yu, J.; Zhang, Q.; Dattilo, D.; Risko, C.; Jones, S. C.; Barlow, S.; Domercq, B.; Amy, F.; Kahn, A.; Bredas, J.-L.; Kippelen, B.; Marder, S. R. *J. Am. Chem. Soc.* **2005**, *127*, 16358.

(13) Chabinyc, M. L.; Street, R. A.; Northrup, J. E. *Appl. Phys. Lett.* **2007**, *90*, 123508.

(14) Wienk, M. M.; Kroon, J. M.; Verhees, W. J. H.; Knol, J.; Hummelen, J. C.; vanHal, P. A.; Janssen, R. A. J. *Angew. Chem., Int. Ed.* **2003**, *42*, 3371. Yao, Y.; Shi, C.; Li, G.; Shrotriya, V.; Pei, Q.; Yang, Y. *Appl. Phys. Lett.* **2006**, *89*, 153507.

Table 1. Typical Physical and Electronic Properties of Metallated Conjugated Polymers

	λ_{max}[a] (nm)	HOMO[b] (eV)	LUMO[c] (eV)	E_g[d] (eV)	μ_h[e] ($\times 10^{-2}$ cm^2/(V s))	I_{on}/I_{off}
P1	562 (587)	−5.20	−3.35	1.85	0.006 (0.01)	4.8×10^2
P2	566 (592)	−5.18	−3.34	1.84	0.15 (0.25)	5.2×10^4
P3	588 (610)	−5.12	−3.30	1.82	0.57 (0.86)	1.5×10^6
P4	596 (611)	−5.14	−3.33	1.81	0.89 (1.00)	1.5×10^6

[a] In CH_2Cl_2 solution. Film is shown in parentheses. [b] In CH_2Cl_2 (vs SCE) solution (0.1 M Bu_4NPF_6 electrolyte), Pt electrode. Scan rate: 100 mV/s. Fc/Fc^+ internal reference. [c] Calculated by $E_g + E_{HOMO}$. [d] Optical energy gap (absorption edge). [e] Average charge carrier mobility in ambient conditions. The highest value of each system is given in parentheses.

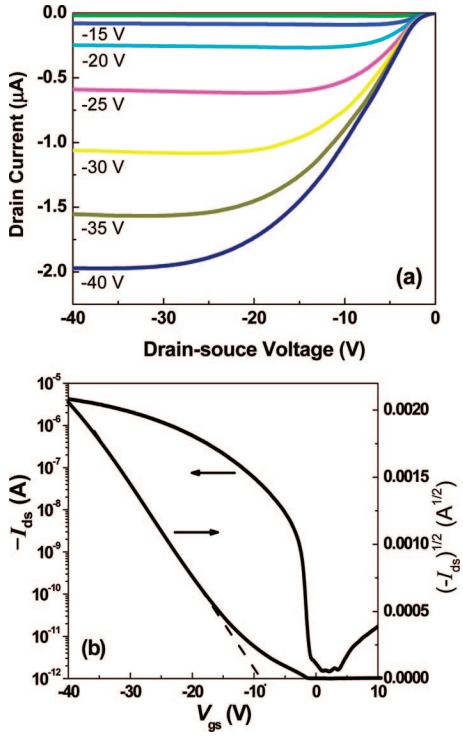

Figure 2. Output (a) and transfer (b) characteristics of P4 OFETs on OTS modified SiO_2 as a function of gate voltage (V_{GS}). ($W = 9000$ μm and $L = 90$ μm).

Table 2. Summary of Device Performance for Various Bulk Heterojunction Polymer Solar Cells

polymer	acceptor[a]	V_{oc} (V)	J_{sc} (mA/cm^2)	FF (%)	PCE[b] (%)
P1	PCBM	0.818	4.22	38.4	1.32 (1.40)
	$PC_{71}BM$	0.828	4.04	45.7	1.53 (1.68)
P2	PCBM	0.839	4.76	38.3	1.53 (1.67)
	$PC_{71}BM$	0.844	7.33	39.6	2.45 (2.69)
P3	PCBM	0.805	5.35	47.2	2.03 (2.15)
	$PC_{71}BM$	0.813	8.67	50.6	3.57 (3.76)
P4	PCBM	0.793	5.67	49.4	2.22 (2.38)
	$PC_{71}BM$	0.787	9.61	49.3	3.73 (4.13)

[a] Active layer thickness of ~80 nm cast from $CHCl_3$ solution (polymer:PCBM or $PC_{71}BM$ = 1:4 w/w ratio). [b] Average power conversion efficiency under AM 1.5 G irradiation at 100 mW/cm^2. The highest value of each system is given in parentheses. All characterizations were performed in an ambient environment.

conditions, the improvement in solar cell performance can be correlated to the improved polymer hole mobility. The best solar cell performance is based on the highest hole mobility polymer (**P4**) and $PC_{71}BM$. The best performance measured for this system leads to an open circuit voltage of $V_{oc} = 0.79$, a short circuit current of $J_{sc} = 10.12$ mA/cm^2, a fill factor of FF = 51.4%, and a power conversion efficiency of PCE = 4.13% under simulated AM 1.5 G illumination.

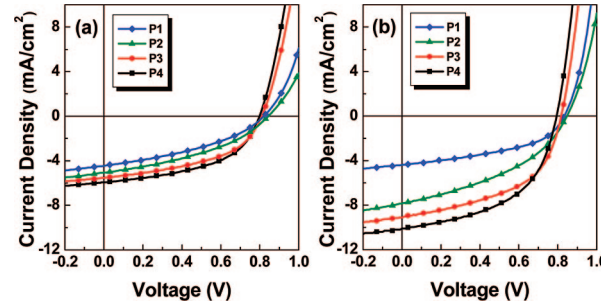

Figure 3. Current−voltage characteristics of bulk heterojuntion solar cells with polymer:PCBM (a) and polymer:$PC_{71}BM$ (b) cast from chloroform solution.

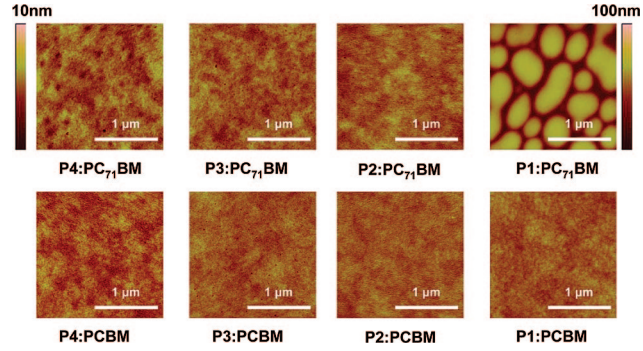

Figure 4. AFM images of polymer:PCBM (1:4) and polymer:$PC_{71}BM$ (1:4) film cast from chloroform.

In additon, post thermal annealing does not further improve the performance of the solar cells due to the amorphous nature of the polymers which are less sensitive to postprocessing when compared to polycrystalline polymers.

In summary, we have designed and synthesized a series of amorphous metallated conjugated polymers exhibiting high field-effect mobilities and high solar cell power conversion efficiencies. The broad absorption and relatively high mobility of these polymers provides the promise of a new class of conjugated materials for all-solution processed field-effect transistors and polymer solar cells.

Acknowledgment. This work was supported by the National Science Foundation's NSF-STC program under DMR-0120967 and the DOE's "Future Generation Photovoltaic Devices and Process" program. A.K.-Y.J.thanks the Boeing-Johnson Foundation for financial support. H.-L.Y. thanks the Intel Foundation Ph.D. Fellowship.

Supporting Information Available: Syntheses and experimental details, device performance, AFM, and XRD images (PDF). This material is available free of charge via the Internet at http://pubs.acs.org.

CM8016424